# Post-growth surface smoothing of thin films of diindenoperylene

A. Hinderhofer,[1,2,a)] T. Hosokai,[3] K. Yonezawa,[2] A. Gerlach,[1] K. Kato,[2] K. Broch,[1] C. Frank,[1] J. Novák,[1,4] S. Kera,[2] N. Ueno,[2] and F. Schreiber[1]
[1]*Institute for Applied Physics, University of Tübingen, Auf der Morgenstelle 10, Tübingen 72076, Germany*
[2]*Graduate School of Advanced Integration Science, Chiba University,1-33 Yayoi-cho, Inage-ku, Chiba 263-8522, Japan*
[3]*Department of Materials and Science, Iwate University, Ueda 4-3-5, Morioka, Iwate 0208551, Japan*
[4]*European Synchrotron Radiation Facility (ESRF), BP 220, Grenoble 38043, France*

(Received 16 April 2012; accepted 29 June 2012; published online 18 July 2012)

We applied *in situ* x-ray reflectivity and ultraviolet photoelectron spectroscopy to study the impact of annealing on low temperature (200 K) deposited organic thin films of diindenoperylene (DIP) on $SiO_2$ and indium tin oxide (ITO). At 200 K, DIP is crystalline on $SiO_2$ and amorphous on ITO. Upon heating to room temperature, the roughness of DIP is reduced on both substrates, from 1.5 nm to 0.75 nm ($SiO_2$) and from 0.90 nm to 0.45 nm (ITO). The smoothing is accompanied by crystallization of the surface molecules, whereas the bulk structure of the films does not strongly reorganize. © *2012 American Institute of Physics*. [http://dx.doi.org/10.1063/1.4737168]

The structure of organic semiconductor thin films is frequently modified by varying the substrate temperature during deposition to tune the electrical and optical characteristics of the films. In general, at high substrate temperatures ($T$), molecular mobilities are high leading to enhanced crystallinity and grain size in the grown films.[1,2] In contrast, deposition at low temperatures is applied to obtain less crystalline or amorphous films.[3–9] For low $T$ growth, it is often not clear, if the film undergoes a structural or morphological transition upon heating to room temperature, because characterization is mostly done after growth at room temperature. In particular, properties like crystallinity, molecular orientation, and roughness of the film surface are important for device applications with organic heterostructures, where the top surface of the first layer serves as a template for subsequent layers.[10–12]

In this letter, we study the morphological and electronic impact of post-growth heating on low $T$ deposited organic thin films by x-ray reflectivity (XRR) and ultraviolet photoelectron spectroscopy (UPS). For the experiments, we choose diindenoperylene (DIP, $C_{32}H_{16}$, inset Fig. 1(b)) as an organic material with high relevance for applications.[13–16] For example, organic solar cells with DIP as electron donor reached high fill factors and power conversion efficiencies.[13] DIP is deposited on two different substrates (indium-tin-oxide (ITO) and silicon dioxide ($SiO_2$)), because the film characteristics on both substrates differ in crystallinity.[6,7] X-ray diffraction techniques[17] were applied to determine the bulk crystal structure and surface roughness ($\sigma_{RMS}$). UPS was used to determine the surface electronic structure, which depends on the crystallinity, orientation, and uniformity of domains at the surface.[18–20] The combination of both techniques, therefore, provides information on the change of structure and morphology of the films for the entire thickness range.

Organic thin films of DIP were grown on silicon wafers with native $SiO_2$ (surface roughness $\sigma_{RMS} = 0.3$ nm) or on ITO-coated glass substrates (ITO thickness: 130 nm, $\sigma_{RMS} = 0.95$ nm) under ultra high vacuum (UHV) conditions (base pressure $< 6 \times 10^{-9}$ mbar) by thermal evaporation. Before deposition, substrates were cleaned ultrasonically

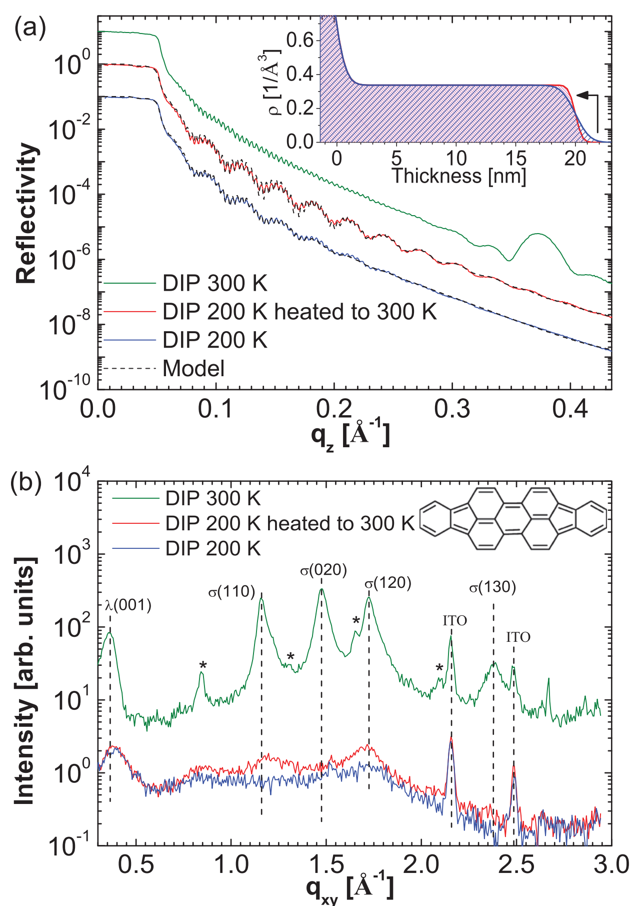


FIG. 1. (a) XRR and (b) GIXD data of a DIP film ($d = 20$ nm) grown on ITO at 200 K measured directly after growth at 200 K and after slow heating (∼1 h) to 300 K. For comparison, data from a film grown and measured at 300 K are also shown. The inset in (a) shows the modeled electron density of the 200 K film directly after growth (blue) and after heating (red). The inset in (b) shows the molecular structure of DIP.

a)Electronic mail: alexander.hinderhofer@chiba-u.jp.

 © 2012 American Institute of Physics

Downloaded 30 Jul 2012 to 134.2.72.186. Redistribution subject to AIP license or copyright; see http://apl.aip.org/about/rights_and_permissions

with acetone, isopropanol, and ultra pure water, followed by heating to 700 K in the UHV growth chamber. The growth rate was between 0.1 and 0.3 nm/min monitored by XRR and a quartz crystal microbalance. Substrate temperatures during growth and measurements were controlled with liquid nitrogen cooling in a range of $T = 200$–$300$ K.

*In situ* XRR and grazing incidence x-ray diffraction (GIXD) for the ITO samples were performed at beamline ID10B ($\lambda = 0.092$ nm) of the ESRF in Grenoble, France. XRR for $SiO_2$ samples were performed at the X04SA beamline of the Swiss Light Source, Paul Scherrer Institut, Villigen, Switzerland ($\lambda = 0.10$ nm). Peak indexing of DIP is based on the crystal structure (P21/a polymorph) reported in Ref. 21. Modeling of XRR data was done with Motofit.[22]

He I UPS experiments were performed with a home-built UHV system equipped with a PHOIBOS-HSA100 analyzer with an energy resolution of 60 meV.[23] UPS were measured at a light incident angle of 45° and electron emission angles of 0° (normal emission). After growth in a UHV preparation chamber, the samples were transferred to the measurement chamber without breaking the vacuum and with keeping the substrate temperature at 200 K. The vacuum level (VL) was obtained by applying a sample bias of −5 V during the UPS measurements.

Fig. 1(a) shows XRR data from a DIP film with a thickness of $d = 20$ nm grown on ITO at 200 K and measured at 200 K directly after growth and after slow heating (∼1 h) to 300 K. Both films show no out-of-plane Bragg reflections, indicating weak order in this direction. We applied a three layer model (glass-ITO-DIP) to fit the electron densities $\rho$ of the as-grown and the annealed films (inset Fig. 1(a)). From the electron densities of both films, it is evident that the roughness is reduced by 50% during annealing from initially $\sigma_{RMS} = 0.90$ nm to $\sigma_{RMS} = 0.45$ nm at 300 K. For comparison, XRR from a film grown and measured at 300 K is also shown. This film is crystalline and exhibits an out-of-plane lattice spacing of 1.69 nm corresponding to textured growth of the strained high temperature phase of DIP (HT-phase)[21,24] with the (001) plane parallel to the substrate ($\sigma$-structure). The roughness of this film is significantly higher compared to low $T$ deposited films ($\sigma_{RMS} = 2.6$ nm).

Fig. 1(b) shows GIXD data of the 200 K DIP film on ITO before and after heating. Before heating, the film shows only very broad Bragg reflections with the most intense feature stemming from domains with nearly lying DIP molecules ($\lambda$(001) of the HT-phase). During heating, the film crystallizes partly in the DIP HT-phase as seen by the slight intensity increase of the $\sigma$(110) and $\sigma$(120) reflections. However, all reflections both from the $\lambda$- and $\sigma$-structure remain broad with a coherent island size of less than 5 nm estimated with the Scherrer formula.[17] GIXD data from a crystalline film grown and measured at 300 K (Fig. 1(b)) exhibit mainly Bragg reflections corresponding to textured growth of the DIP HT-phase ($\sigma$-structure).[21] Bragg reflections marked with stars stem presumably from a DIP low temperature phase as suggested in Refs. 6, 7, and 21. XRR and GIXD data show that during heating to room temperature, the bulk DIP film on ITO crystallizes only weakly, however, the reorganization of the surface molecules yield a very low roughness.

In the context of the present study, a reduced surface roughness of the substrate has a similar effect on the growth as a higher substrate temperature. A rough surface has deeper traps in the surface potential and reduces therefore effectively the diffusion length of the molecules. On a smooth substrate, we observe for DIP therefore less nucleation of domains with $\lambda$-orientation (HT-phase) and of low temperature phases and overall better crystallinity. This was demonstrated in Ref. 6, where DIP deposited on smooth $SiO_2$ yields films, which are crystalline even at low $T$. In the following, we report an *in situ* study of a low $T$ deposited DIP film on $SiO_2$, in order to test if the surface smoothing observed for amorphous DIP on ITO is also present for crystalline films upon heating to room temperature.

Figure 2 shows XRR data from a DIP film ($d = 10$ nm) grown on $SiO_2$ at 200 K measured at 200 K directly after growth and after slow heating to 300 K. From the modeled electron densities of the heated and the as-grown 200 K DIP film (inset Fig. 2), we find that both films are crystalline and exhibit an out-of-plane lattice spacing of 1.69 nm corresponding again to textured growth of the strained DIP HT-phase ($\sigma$-structure).[21,24] However, the layer fillings of these films show significant differences (inset Fig. 2), resulting in roughnesses of $\sigma_{RMS} = 1.5$ nm for the as-grown film and $\sigma_{RMS} = 0.75$ nm for the heated film. This observation is rationalized by a molecular "downhill" current from the top layer (7th) to the partly filled lower lying layers (6th, 5th, 4th), thereby leaving the out-of-plane crystal structure and the intermediate electron density unchanged. For comparison, XRR from a film grown and measured at 300 K is also shown. This film has the same out-of-plane lattice spacing (1.69 nm) and a similar roughness as the 200 K film without annealing ($\sigma_{RMS} = 1.6$ nm).

The observation of the roughness reduction by ∼50% shows that the reorganization of surface molecules is not exclusively a feature of amorphous films. Surprisingly, also for a bulk crystalline film deposited at low $T$, the surface is smoothed upon heating.

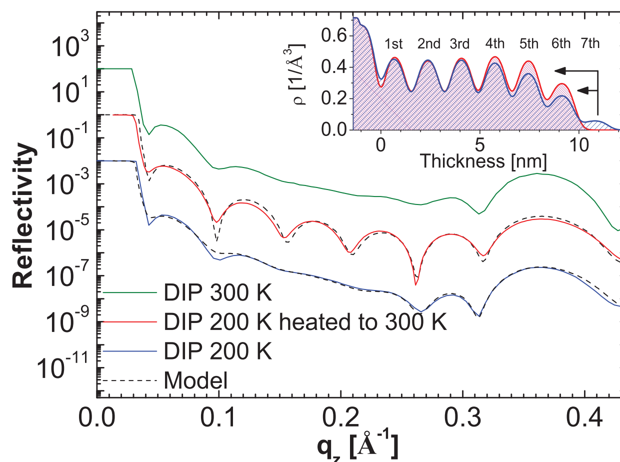


FIG. 2. XRR data of DIP films ($d = 10$ nm) grown on $SiO_2$ at two different substrate temperatures (200 K and 300 K). For the 200 K DIP film, XRR data directly after growth at 200 K are shown together with data after slow heating (∼1 h) to 300 K. The inset shows the modeled electron density of the 200 K film directly after growth (blue) and the heated 200 K film (red).

Downloaded 30 Jul 2012 to 134.2.72.186. Redistribution subject to AIP license or copyright; see http://apl.aip.org/about/rights_and_permissions

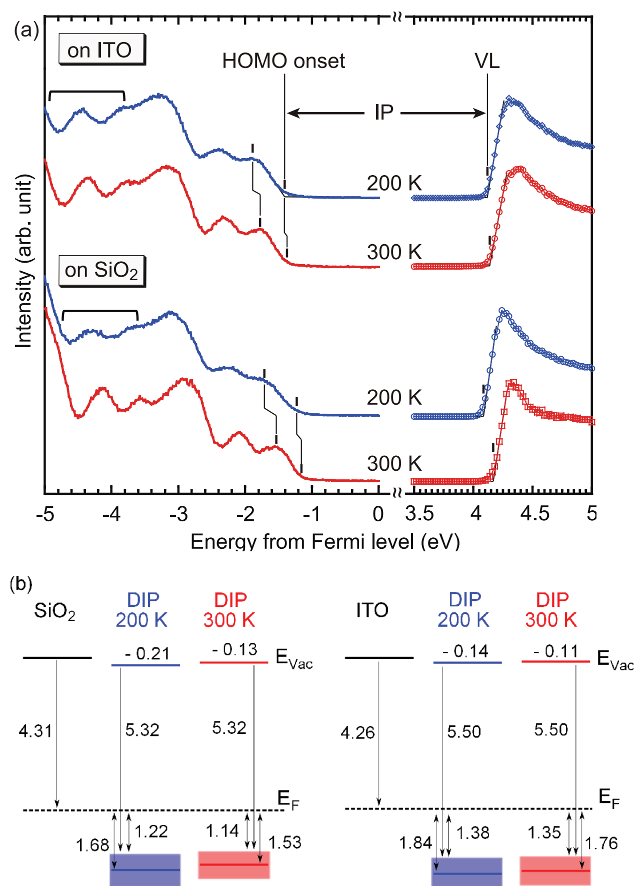


FIG. 3. (a) UPS data of DIP films grown on $SiO_2$ ($d = 10$ nm) and ITO ($d = 20$ nm) at 200 K and after slow heating (~4 h) to 300 K. (b) Schematic energy level diagram. The HOMO width is given by the difference of the HOMO peak position and the HOMO onset.

We employed UPS to detect the correlation between structure and the molecular electronic states upon heating, since the electronic states near the surface play a significant role in the energy level alignment of organic heterostructures. The probing depth of UPS is ~1 nm, which means that the bulk of the film does not contribute to the measured data. Fig. 3 shows UPS data of DIP films prepared under similar conditions as those as presented above. The ionization potential (IP) of DIP (200 K) on $SiO_2$ (5.32 eV) and on ITO (5.5 eV) was determined from the onset of the highest occupied molecular orbital (HOMO) and the VL. The IP of DIP depends on the orientation of the molecules at the surface.[25] An IP of 5.32 eV is consistent with a nearly upright oriented DIP film.[13,26] The IP of lying DIP is larger by ~0.4 eV compared to nearly upright standing DIP as was shown in Refs. 27–29. The DIP film on ITO is nearly amorphous and exhibits therefore no preferred molecular orientation. In addition, the size of orientational domains is very small, which results in a common vacuum level. Consistently, the IP of 5.5 eV of this film corresponds to an average of standing and lying DIP.

After heating, the IP of both films did not change significantly, indicating that the DIP molecules did not reorient on average. However, we detect a parallel shift of all valence features towards the Fermi level, which is attributed partly to an interfacial dipole effect and partly to the reduction of gap states (Fig. 3(b)). Dipole effects are associated with a parallel shift of the HOMO and the vacuum level. A HOMO shift stemming from a reduction of gap states is recognized by a reduced peak width of the valence states (gap state effect). For DIP on $SiO_2$ (ITO), the HOMO shift is $\Delta E = 0.15$ eV ($\Delta E = 0.08$ eV) with a contribution of 0.08 eV (0.03 eV) from the dipole effect and 0.07 eV (0.05 eV) from the gap state effect. The dipole effect may be attributed either to an interfacial dipole between the surface layer and its underlayer induced by a slightly different electron density at the interface,[30] and/or a temperature dependent level alignment between the substrates and the DIP. The spectral broadening at low $T$ is caused by different polarization environments associated with disorder of the molecules at the nearest-neighbor level. The peak narrowing upon heating indicates therefore that the surface molecules are more uniformly ordered for both systems which results in more similar polarization environments for them. Since the density of gap states is reduced, the HOMO level shifts closer to the Fermi level. This effect is explained in detail in Refs. 31–33.

When comparing the DIP-on-$SiO_2$ and the DIP-on-ITO systems, several differences can be found: First, at 200 K, molecules at the film surface on $SiO_2$ orient basically nearly upright ($\sigma$-orientation), which is consistent with the data in Fig. 1. Nevertheless, at this temperature, the spectral features of DIP-on-$SiO_2$ exhibit a similar or even stronger broadening compared to DIP-on-ITO, which can be observed most easily from the energy region around $-4$ eV marked with brackets in Fig. 3. The broad spectrum of DIP-on-$SiO_2$ implies that, in spite of better bulk crystallinity, the surface material in films on $SiO_2$ does not show a better in-plane order than DIP-on-ITO. Second, upon heating peak narrowing and the spectral shift are both significantly more pronounced for the DIP-on-$SiO_2$ system compared to the DIP-on-ITO system. This implies that the ordering effect of the surface material is more pronounced if the crystallinity of the bulk material is better, which is the case for DIP-on-$SiO_2$.

In summary, we observed the surface smoothing of low $T$ deposited organic thin films upon heating to room temperature. With the combined results from x-ray diffraction and UPS, we illustrate the process of surface smoothing by crystallization as in Fig. 4. After low $T$ deposition on ITO, the DIP film is nearly amorphous and also rough. Upon heating the surface material is crystallizing in domains without any predominant texture, whereas the bulk material does not strongly reorganize, because of lower mobility of these molecules. This crystallization process is associated with a molecular "downhill" current, which smooths the surface. In contrast to deposition on ITO, the DIP film deposited on $SiO_2$ is, except for the top surface material, already crystalline with a preferred orientation of the domains ($\sigma$-orientation). Upon heating to room temperature, the surface material is also crystallizing and exhibits thereby a similar smoothing as the film on ITO. Therefore, we conclude that the smoothing effect observed is qualitatively similar irrespective of the degree of bulk crystallinity. In addition, due to the crystallization, the density of gap states at the surface is changed leading to a shift of the valence band features towards the Fermi level. The observed post-growth smoothing and crystallization is of importance for the growth of organic heterostructures, where the top surface of the first layer serves as a template for subsequent layers.

Downloaded 30 Jul 2012 to 134.2.72.186. Redistribution subject to AIP license or copyright; see http://apl.aip.org/about/rights_and_permissions

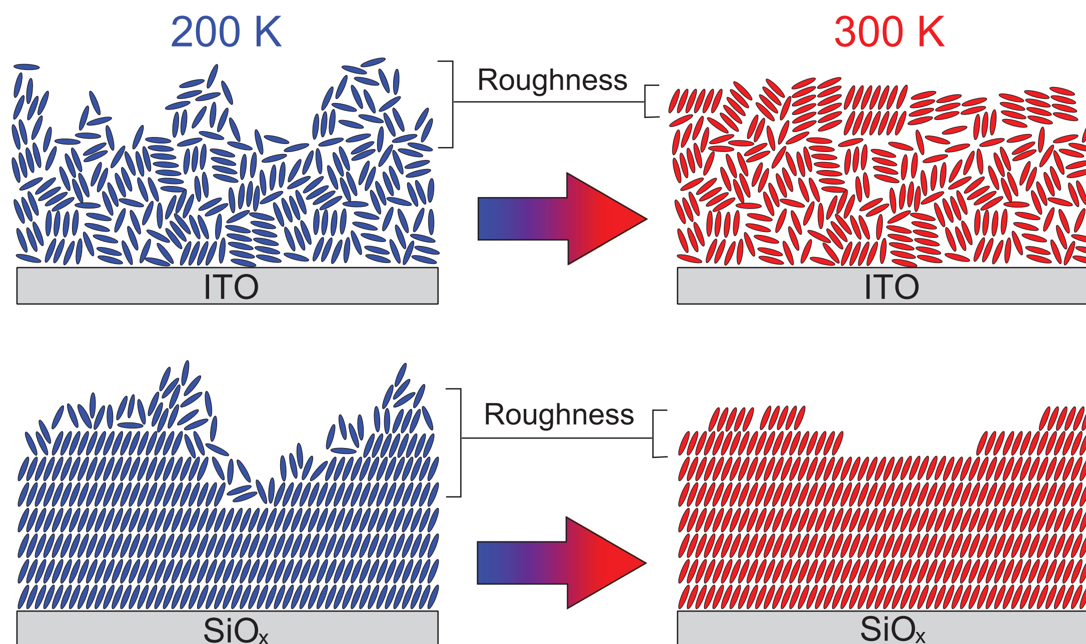


FIG. 4. A sketch of DIP thin films on ITO and $SiO_2$ illustrating the surface smoothing due to crystallization upon heating.

The authors thank F. Bussolotti and S. Duhm for helpful discussions and P. Willmott and S. Leake at the Swiss Light Source whose great efforts have made these experiments possible. This research project has been supported by the DFG, the Global-COE Program of MEXT (G03) at Chiba University and by the European Commission under the 7th Framework Programme: Grant Agreement Number 226716. A.H. acknowledges support from the JSPS.

[1]G. Witte and C. Wöll, J. Mater. Res. **19**, 1889 (2004).
[2]*Physics of Organic Semiconductors*, edited by W. Brütting (Wiley-VCH, Weinheim, 2005).
[3]D. Käfer, C. Wöll, and G. Witte, Appl. Phys. A **95**, 273 (2009).
[4]C. D. Dimitrakopoulos and P. R. L. Malenfant, Adv. Mater. **14**, 99 (2002).
[5]K. Walzer, B. Maennig, M. Pfeiffer, and K. Leo, Chem. Rev. **107**, 1233 (2007).
[6]S. Kowarik, A. Gerlach, S. Sellner, L. Cavalcanti, O. Konovalov, and F. Schreiber, Appl. Phys. A **95**, 233 (2009).
[7]A. Hinderhofer, T. Hosokai, C. Frank, J. Novák, A. Gerlach, and F. Schreiber, J. Phys. Chem. C **115**, 16155 (2011).
[8]R. Matsubara, M. Sakai, K. Kudo, N. Yoshimoto, I. Hirosawa, and M. Nakamura, Org. Electron. **12**, 195 (2011).
[9]B. Krause, F. Schreiber, H. Dosch, A. Pimpinelli, and O. H. Seeck, Europhys. Lett. **65**, 372 (2004).
[10]A. Hinderhofer and F. Schreiber, ChemPhysChem **13**, 628 (2012).
[11]J. Yang and D. Yan, Chem. Soc. Rev. **38**, 2634 (2009).
[12]A. Hinderhofer, A. Gerlach, S. Kowarik, F. Zontone, J. Krug, and F. Schreiber, Europhys. Lett. **91**, 56002 (2010).
[13]J. Wagner, M. Gruber, A. Hinderhofer, A. Wilke, B. Bröker, J. Frisch, P. Amsalem, A. Vollmer, A. Opitz, N. Koch, F. Schreiber, and W. Brütting, Adv. Funct. Mater. **20**, 4295 (2010).
[14]U. Hörmann, J. Wagner, M. Gruber, A. Opitz, and W. Brütting, Phys. Status Solidi (RRL) **5**, 241 (2011).
[15]M. Horlet, M. Kraus, W. Brütting, and A. Opitz, Appl. Phys. Lett. **98**, 233304 (2011).
[16]D. Kurrle and J. Pflaum, Appl. Phys. Lett. **92**, 133306 (2008).
[17]M. Birkholz, *Thin Film Analysis by X-Ray Scattering* (Wiley-VCH, Weinheim, 2006).
[18]N. Ueno and S. Kera, Prog. Surf. Sci. **83**, 490 (2008).
[19]H. Ishii, K. Sugiyama, E. Ito, and K. Seki, Adv. Mater. **11**, 605 (1999).
[20]N. Koch, ChemPhysChem **8**, 1438 (2007).
[21]M. A. Heinrich, J. Pflaum, A. K. Tripathi, W. Frey, M. L. Steigerwald, and T. Siegrist, J. Phys. Chem. C **111**, 18878 (2007).
[22]A. Nelson, J. Appl. Crystallogr. **39**, 273 (2006).
[23]T. Hosokai, M. Horie, T. Aoki, S. Nagamatsu, S. Kera, K. K. Okudaira, and N. Ueno, J. Phys. Chem. C **112**, 4643 (2008).
[24]S. Kowarik, A. Gerlach, S. Sellner, F. Schreiber, L. Cavalcanti, and O. Konovalov, Phys. Rev. Lett. **96**, 125504 (2006).
[25]S. Duhm, G. Heimel, I. Salzmann, H. Glowatzki, R. L. Johnson, A. Vollmer, J. P. Rabe, and N. Koch, Nature Mater. **7**, 326 (2008).
[26]A. Wilke, P. Amsalem, J. Frisch, B. Brker, A. Vollmer, and N. Koch, Appl. Phys. Lett. **98**, 123304 (2011).
[27]Y. L. Huang, W. Chen, H. Huang, D. C. Qi, S. Chen, X. Y. Gao, J. Pflaum, and A. T. S. Wee, J. Phys. Chem. C **113**, 9251 (2009).
[28]A. C. Dürr, N. Koch, M. Kelsch, A. Ruehm, J. Ghijsen, R. L. Johnson, J.-J. Pireaux, J. Schwartz, F. Schreiber, H. Dosch, and A. Kahn, Phys. Rev. B **68**, 115428 (2003).
[29]J. Q. Zhong, H. Y. Mao, R. Wang, D. C. Qi, L. Cao, Y. Z. Wang, and W. Chen, J. Phys. Chem. C **115**, 23922 (2011).
[30]H. Yamane, Y. Yabuuchi, H. Fukagawa, S. Kera, K. K. Okudaira, and N. Ueno, J. Appl. Phys. **99**, 093705 (2006).
[31]T. Sueyoshi, H. Kakuta, M. Ono, K. Sakamoto, S. Kera, and N. Ueno, Appl. Phys. Lett. **96**, 093303 (2010).
[32]H. Y. Mao, F. Bussolotti, D.-C. Qi, R. Wang, S. Kera, N. Ueno, A. T. S. Wee, and W. Chen, Org. Electron. **12**, 534 (2011).
[33]T. Hosokai, H. Machida, A. Gerlach, S. Kera, F. Schreiber, and N. Ueno, Phys. Rev. B **83**, 195310 (2011).

Downloaded 30 Jul 2012 to 134.2.72.186. Redistribution subject to AIP license or copyright; see http://apl.aip.org/about/rights_and_permissions